Letter

Bull. Volcanol. Soc. Japan
Vol. 60 (2015) No. 2, pp. 241–249

Multiple Vent-forming Phreatic Eruptions after AD 1663 in the Noboribetsu Geothermal Field, Kuttara Volcano, Hokkaido, Japan

Yoshihiko GOTO*, Yoshimasa TORIGUCHI*, Hirotaka SASAKI* and Akira HATAKEYAMA*

(Received July 8, 2014; Accepted February 2, 2015)

The Noboribetsu geothermal field (area 1×1.5 km) is located in the western part of Kuttara volcano, southwestern Hokkaido, Japan. Seventy-one shallow trenches (<90 cm deep) were systematically dug within the geothermal field, in order to study the stratigraphy and distribution of the most recent phreatic fall deposit (the Nb-a deposit) erupted from the field. The Nb-a deposit (<68 cm thick) consists of altered dacitic lithic clasts in a fine-grained clay-rich matrix. The deposit overlies the Us-b tephra that was emplaced in AD 1663. Stratigraphic sections constructed from the 71 trenches indicate that the deposit is distributed within an elliptical area measuring 850×1250 m across and extending NNW-SSE. Isopach and maximum-grain-size isopleth maps indicate that the deposit increases in thickness and maximum-grain-size toward several explosion craters. These data suggest that phreatic eruptions, through multiple vents, occurred in the Noboribetsu geothermal field after AD 1663.
Key words: phreatic eruption, deposit, trench survey, Noboribetsu geothermal field, Kuttara volcano

1. Introduction

The Noboribetsu geothermal field at Kuttara volcano, southwestern Hokkaido is one of major geothermal fields in Japan (Fig. 1). Geological and geochronological studies (Goto *et al*., 2011a, b, 2013; Katsui *et al*., 1988; Yamazaki, 1986) indicate that at least 12 episodes of phreatic eruptions (here, the term 'phreatic eruptions' is used for steam-driven explosions that do not involve fresh magma, following Barberi *et al*., 1992 and McPhie *et al*., 1993) have occurred in this field within the past 8500 years. However, the details of each episode, such as the mode and magnitude of eruptions, remain unclear. We performed a stratigraphic survey of the most recent phreatic fall deposit erupted in this field (the Nb-a deposit; Goto *et al*., 2013) in order to clarify the style of the most recent phreatic eruptions in this field. As this field is generally covered with thick vegetation, we excavated and examined 71 shallow trenches throughout the field. This paper reports the results of the stratigraphic survey and discusses the style of the most recent eruptions.

2. Noboribetsu geothermal field

The Noboribetsu geothermal field lies in the western part of Kuttara volcano (Fig. 1) and is approximately 1 km wide (ENE-WSW) and 1.5 km long (NNW-SSE) (Katsui *et al*., 1988; Moriizumi, 1998). This field is inferred to have formed at *ca.* 15 ka (Goto and Danhara, 2011; Goto *et al*., 2013), and is characterized by a dacitic cryptodome (Hiyoriyama cryptodome), a volcanic lake (Oyunuma Lake), and a fumarolic valley (Jigokudani Valley) (Figs. 2 and 3). The Hiyoriyama cryptodome, in the northern part of the geothermal field, is 350–550 m in diameter and rises 130 m above the surrounding areas (Fig. 2A; Goto and Johmori, 2013). Oyunuma Lake (115×210 m in area), located in the central part of the geothermal field, is the largest explosion crater in the field and is filled with hot acidic water (Fig. 2A). The Jigokudani Valley, in the southern part of the geothermal field, extends for 500 m in an ENE-WSW orientation and hosts active fumaroles (Fig. 2B). The geothermal manifestations of the geothermal field (active fumaroles, hot springs, and hydrothermal alteration zones) are distributed in a zone extending NNW-SSE from the Hiyoriyama cryptodome to the Jigokudani Valley (Goto and Johmori, 2011). A number of small explosion craters (diameter 25–210 m) occur in this zone (Goto *et al*., 2011a).

3. Trench survey

The Noboribetsu geothermal field is generally covered by forests consisting of tall trees and short bamboo, except in areas where geothermal manifestations occur (Fig. 2A). Stratigraphic and descriptive studies of the Nb-a deposit are thus hampered by limited exposures caused by a thick cover of vegetation. To address this issue, 71 shallow trenches were systematically dug throughout the Noboribetsu geothermal field (Fig. 3). The trenches were excavated using a hand shovel. Each trench had a horizontal area of

*College of Environmental Technology, Graduate School of Engineering, Muroran Institute of Technology, Mizumoto-cho 27–1, Muroran, Hokkaido 050–8585, Japan.

Corresponding author: Yoshihiko Goto
e-mail: ygoto@mmm.muroran-it.ac.jp

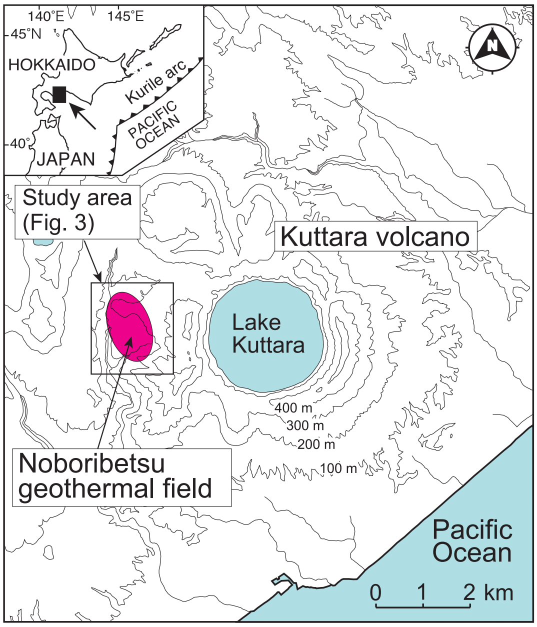

Fig. 1. Location of the Noboribetsu geothermal field in the western part of Kuttara volcano, Hokkaido, Japan.

Fig. 2. Photographs of the Noboribetsu geothermal field. (A) The Hiyoriyama cryptodome and Oyunuma Lake, viewed from the south. Road for scale. (B) The Jigokudani Valley viewed from the east. The valley contains active fumaroles.

50×50 cm and was <90 cm deep (Fig. 4).

4. Stratigraphic sections

Figure 5 shows stratigraphic sections obtained from the 71 trenches. The sections indicate that the Nb-a deposit overlies the Us-b tephra (>60 cm thick; Machida and Arai, 2003; Yokoyama *et al.*, 1973) and is covered by surface soil (5–20 cm thick). The maximum thickness of the Nb-a deposit is 68 cm (Loc. 16). A thin (<5 mm) soil layer occurs at several locations between the Nb-a deposit and the Us-b tephra (as observed at trench Locs. 1, 7, 8, 10–14, 17–20, 25, 38–43, 57, 60). The Us-b tephra was erupted from Usu volcano of southwestern Hokkaido in AD 1663 (Yokoyama *et al.*, 1973).

The Nb-a deposit occurring in the Jigokudani Valley, observed in trench location 1 (Fig. 3), is representative of the 71 trench sites and is therefore described in detail below. At this location, the Nb-a deposit (40 cm thick) is light yellow, massive (non-stratified), matrix supported, poorly sorted, and composed of subangular to subrounded lithic clasts (up to 30 cm across) within a fine-grained matrix (Fig. 4). The lithic clasts consist mainly of intensely altered dacite. No juvenile magmatic pyroclasts (fresh pumice or scoria) are observed. The matrix of the deposit is clay-rich, cohesive, and composed of altered dacitic lithic fragments, altered pumice fragments, mineral fragments (plagioclase, quartz, hypersthene, hornblende, augite, and opaque minerals), and weathered volcanic glass.

The Us-b tephra at this location comprises a pumice fall deposit, >40 cm thick (Fig. 4). It is pale brown, clast-supported, poorly stratified, and consists of white to pale brown pumice clasts (1–3 cm in size). The pumice consists of fresh volcanic glass and crystals of plagioclase, hypersthene, augite, hornblende, opaque minerals, and apatite. The refractive index of volcanic glass (as analyzed using an RIMS2000 apparatus at Kyoto Fission-Track Co. Ltd.; Danhara *et al.*, 1992) ranges from 1.4887 to 1.4921 (mean, 1.4905; mode, 1.491).

5. Lateral variations in the Nb-a deposit

The Nb-a deposit at all 71 trench sites is generally identical in texture. In detail, however, the Nb-a deposit shows slightly variable textures among the trench sites. For example, in the Jigokudani Valley (Loc. 1) and at most locations, the deposit consists of one fall unit, whereas at some locations (*e.g.*, Loc. 21) the deposit comprises two fall units that can be distinguished by slight changes in color. These fall units are not easily identifiable in the trenches, and are difficult to correlate from one trench to

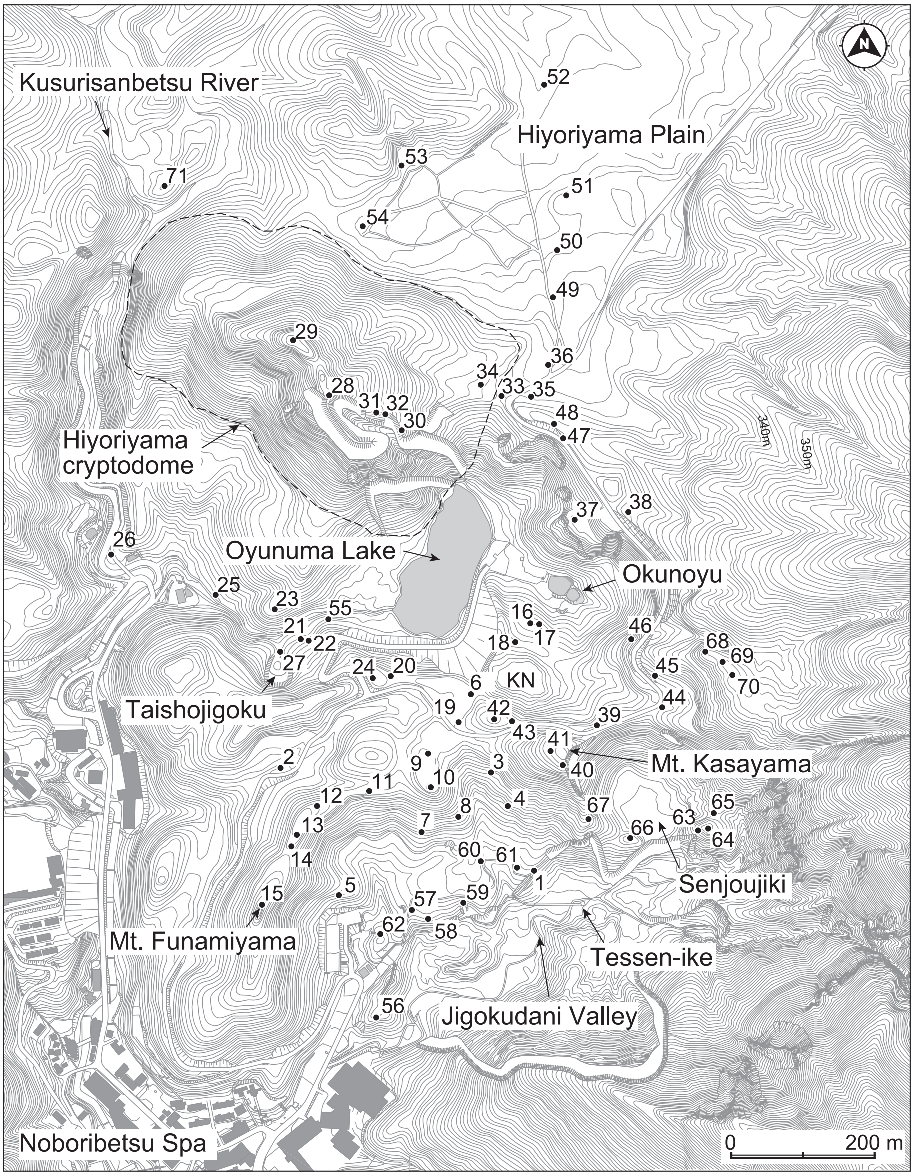

Fig. 3. Topographic map showing the locations of trench sites (numbered 1 to 71) excavated for stratigraphic studies. Stratigraphic sections of each trench site are provided in Fig. 5. KN, Kasayama North crater. Contour intervals are 2 m.

another; consequently, they are not presented in the stratigraphic sections given in Fig. 5.

The Nb-a deposit also varies slightly in component among the trench sites. At the Jigokudani Valley (Loc. 1) and at most other locations, the deposit consists of intensely altered dacitic lithic clasts in a fine-grained clay-rich matrix, whereas at the Hiyoriyama cryptodome (Locs. 30–32) it consists of fresh to altered dacitic lithic clasts and minor andesitic lithic clasts, embedded in a fresh to altered, fine-grained matrix. Such variations are also difficult to correlate between trenches.

6. Grain-size distributions and alteration minerals of the Nb-a deposit

Figure 6 shows grain-size distributions of the Nb-a deposit sampled from various trench sites (Locs. 1, 6, 16, and 31). The samples (each 1–2 kg) were sieved at intervals of 1ϕ (where $\phi = -\log_2 d$, with d being the grain size in millimeters), using a set of sieves ranging from -6ϕ to 4ϕ (64 mm to 1/16 mm). The sieving was carried out in a

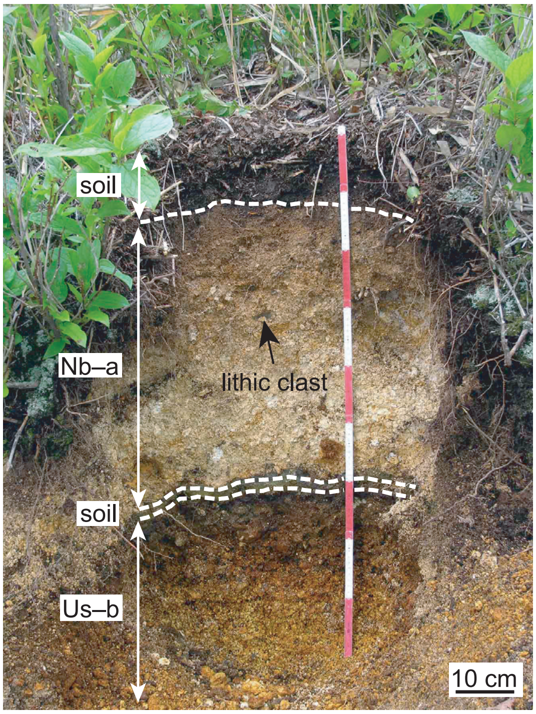

Fig. 4. Photograph of the Nb–a deposit (Nb–a) on the northern slope of the Jigokudani Valley (Loc. 1 in Fig. 3; latitude 42° 29′ 55″ N, longitude 141° 08′ 56″ E). The Nb–a deposit is located 10 cm beneath the ground surface. The deposit consists of altered dacitic lithic clasts (indicated by an arrow) within a fine-grained clay-rich matrix. The deposit overlies the Us–b tephra (Us–b), which was emplaced in AD 1663.

water bath because the samples were cohesive. The sieved samples were dried and weighed to an accuracy of 0.01 g. The grain-size distributions indicate that the Nb-a deposit generally contains a large proportion of grains smaller than 4ϕ (1/16 mm).

Table 1 lists the results of X-ray diffraction (XRD) analyses of the Nb-a deposit from various trench sites (Locs. 1, 6, 16, and 31). The XRD analyses were performed for the $<2\,\mu$m fraction of the matrix of the Nb-a deposit. The $<2\,\mu$m fraction sample was separated by hydraulic elutriation and prepared as oriented samples on glass slides. The XRD analyses were carried out at Okayama University of Science using a Geigerflex RAD-B diffractometer (Rigaku Corporation) with settings of 40 kV, 60 mA, and a scan speed of 2.0° per minute. An ethylene glycol treatment was used to identify smectite. The analyses indicate a variable assemblage of alteration minerals (*e.g.*, smectite, kaolinite, pyrophyllite) among the samples.

7. Distribution and volume of the Nb-a deposit

Figures 7 and 8 show the distributions of the thickness and maximum grain size of the Nb-a deposit, respectively. The maximum grain size at each location was calculated using the average long-axis diameter of the three largest lithic clasts in each trench. These data indicate that the Nb-a deposit is distributed in an ellipsoidal area, measuring 850 × 1250 m across and elongate NNW-SSE. The deposit increases in thickness and grain size toward several explosion craters: Hiyoriyama Summit, Oyunuma, Kasayama North, Okunoyu, and Tessen-ike (Figs. 7 and 8; crater names are after Goto *et al*., 2011a). The isopachs of the deposit around Oyunuma, Kasayama North and Okunoyu are complicated (Fig. 7). The bulk volume of the Nb-a deposit is 4.6×10^5 m^3, as calculated using the method proposed by Hayakawa (1985), based on a 10 cm isopach.

8. Discussion

The Nb-a deposit consists of altered lithic clasts in a clay-rich, fine-grained matrix, and contains no juvenile magmatic pyroclasts (Fig. 4), suggesting it was produced by phreatic explosions. The grain-size distribution of the deposit, which generally show a dominance of grains smaller than 4ϕ (Fig. 6), and the presence of clay minerals (*e.g.*, smectite and kaolinite; Table 1) are consistent with the deposit originating from phreatic explosions. The presence of large lithic clasts (up to 30 cm in length) strongly suggests that the deposit was erupted from within the Noboribetsu geothermal field. This interpretation is consistent with the presence of many small explosion craters in the field (Goto *et al*., 2011a).

The distributions of the thickness and maximum grain size of the Nb-a deposit (Figs. 7 and 8) suggest that the deposit was erupted from several explosion craters (Hiyoriyama Summit, Oyunuma, Kasayama North, Okunoyu, and Tessen-ike). The complicated isopachs around Oyunuma, Kasayama North and Okunoyu (Fig. 7) may be attributed to overlapping of phreatic deposits erupted from these craters. This inference is consistent with the well-preserved morphology of these explosion craters (Goto *et al*., 2011a). The explosion craters are aligned NNW-SSE, extending from the Hiyoriyama cryptodome to the Jigokudani Valley, and their distribution suggests that phreatic eruptions, through multiple vents, occurred within this zone. Lateral variations in the texture and component of the Nb-a deposit may be attributed to the different locations of the many source vents that were active during the phreatic eruption. The variable assemblage of alteration minerals of the Nb-a deposit (Table 1) may also be attributed to the many source vents. Similar phreatic eruptions with multiple vents have been reported from the 1910 and 2000 eruptions of Usu volcano, southwestern Hokkaido, Japan (Ui *et al*., 2002; Yokoyama *et al*., 1973).

The isopach and maximum-grain-size isopleth maps of the Nb-a deposit (Figs. 7 and 8) also suggest that the deposit

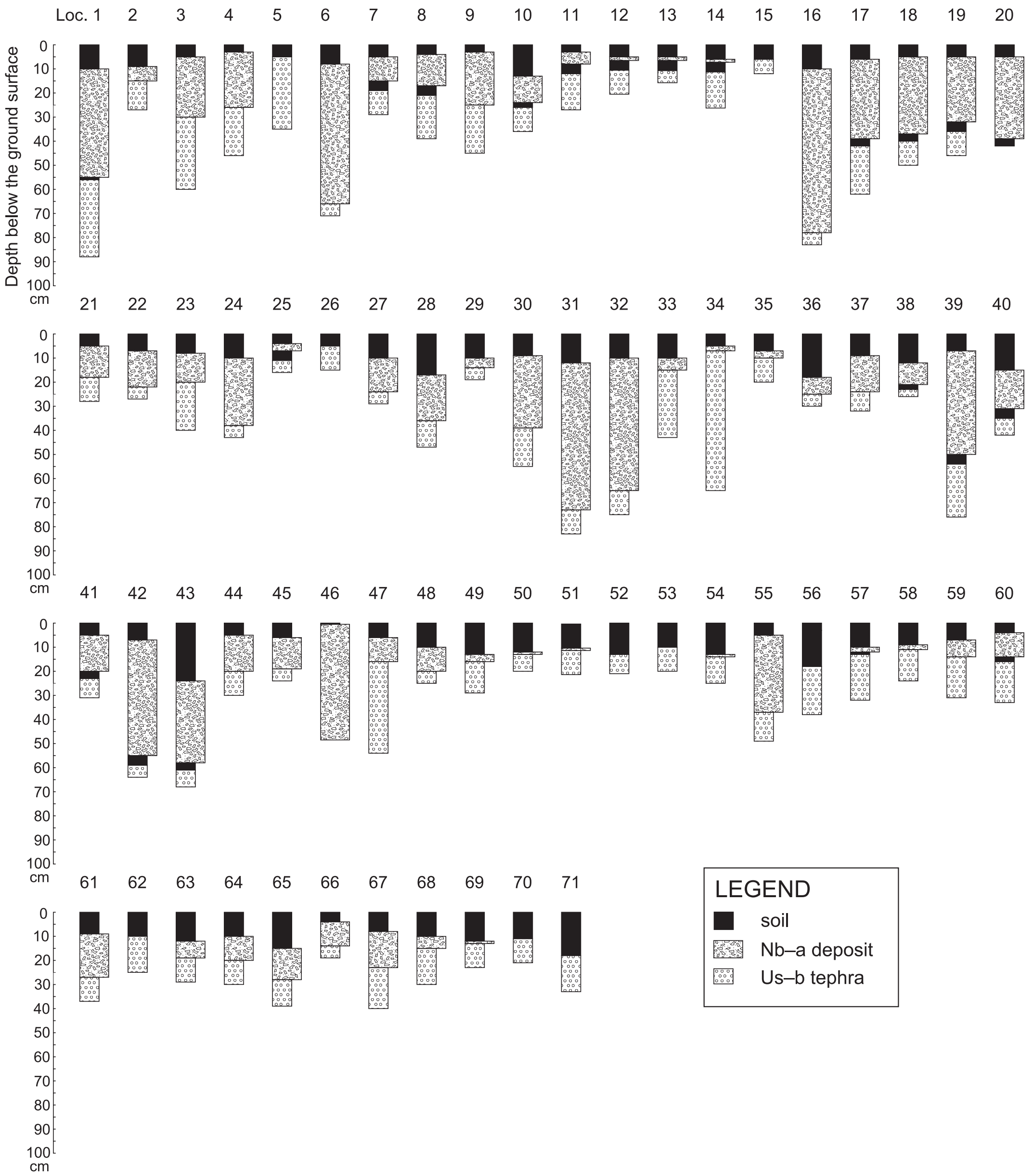

Fig. 5. Stratigraphic sections of the Nb–a deposit obtained from the trenches. Location numbers of the sections correspond to those in Fig. 3.

Table 1. Results of X-ray diffraction (XRD) analyses of the <2 μm fraction of the Nb-a deposit, sampled from locations 1, 6, 16, and 31. The modal abundance of each mineral is classified as abundant (+++), moderate (++), or trace (+).

Location	Sample No.	Smectite	Kaolinite	Pyrophyllite	Quartz	Plagioclase	Opal	Heulandite	Alunite	Jarosite	Gypsum
1	Nb-72	+++	+++				++	++	++	++	
6	Nb-95	+++	++		++		++	+		+++	
16	Nb-94a	+++	+	+	++	+	++		++	+++	
31	Nb-76			+	++	+	+		+		+++

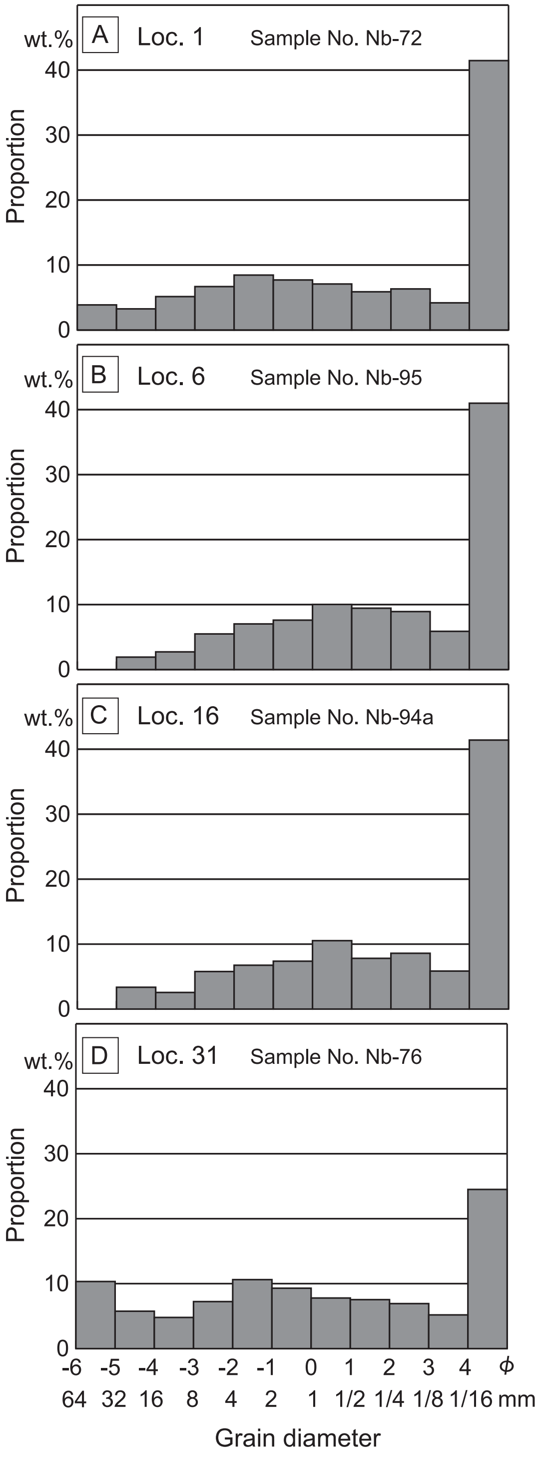

Fig. 6. Grain-size histograms of the Nb-a deposit for samples from locations 1 (A), 6 (B), 16 (C), and 31 (D).

consists of several fall units that originated from different craters. Previous workers have described two such fall units. Katsui *et al*. (1988) described a phreatic fall deposit (the Shinki-Jigokudani pyroclastic fall deposit) from the Jigokudani Valley. Goto *et al*. (2011b) reported a phreatic fall deposit (the Hiyoriyama-a phreatic deposit) from the Hiyoriyama cryptodome. Both units occur above the Us-b tephra, indicating they correspond to the Nb-a deposit. Our results suggest that both the Shinki-Jigokudani and the Hiyoriyama-a deposits represent subunits of the Nb-a deposit that originated from the Tessen-ike Crater and the Hiyoriyama Summit Crater, respectively.

The Nb-a deposit overlies, and is therefore younger than, the Us-b tephra inferred to have been emplaced in AD 1663 (Fig. 4; Yokoyama *et al*., 1973). Hence, the phreatic eruptions associated with the Nb-a deposit must have occurred after AD 1663 (Katsui *et al*., 1988). The presence of a soil layer between the Nb-a deposit and the Us-b tephra at several locations indicates that the explosive events occurred after the late 17th century. An examination of historical records (from AD 1845 to the present) revealed no mention of the eruptions. The phreatic eruptions are thus inferred to have occurred between the late 17th century and AD 1845.

9. Conclusions

The most recent phreatic fall deposit that erupted from the Noboribetsu geothermal field (the Nb-a deposit) is distributed in an elliptical area, measuring 850 × 1250 m across. The deposit overlies the Us-b tephra, which was emplaced in AD 1663. The isopach and maximum-grain-size isopleth maps of the Nb-a deposit suggest that phreatic eruptions, through multiple vents, occurred in the Noboribetsu geothermal field after AD 1663. These eruptions resulted in the formation of several explosion craters aligned NNW-SSE. The present results are of value in evaluating the volcanic hazards in the Noboribetsu geothermal field.

Acknowledgements

This research was sponsored by the Ministry of Education, Culture, Sports, Science and Technology of Japan (MEXT), and was supported financially by the Muroran Institute of Technology. We thank T. Danhara (Kyoto Fission-Track Co. Ltd.) for measuring the refractive index of volcanic glass. Comments by Y. Miyabuchi (Kumamoto University), an anonymous referee, and Y. Suzuki (Waseda University) significantly improved the manuscript. A component of this research was performed as part of compiling a hazard map of Kuttara volcano, issued by the City of Noboribetsu.

Fig. 7. Isopach map for the Nb-a deposit. The deposit is distributed in an elliptical area (850 × 1250 m across) that is elongate NNW-SSE. The thickness of the deposit increases toward the following explosion craters: Hiyoriyama Summit (HS), Oyunuma (OY), Kasayama North (KN), Okunoyu (OK), and Tessen-ike (TI) (red areas in the figure). Topographic contour intervals are 2 m.

Fig. 8. Maximum-grain-size isopleth map for the Nb-a deposit. The deposit increases in maximum-grain-size toward the following explosion craters: Hiyoriyama Summit (HS), Oyunuma (OY), Kasayama North (KN), Okunoyu (OK), and Tessen-ike (TI) (red areas in the figure). Topographic contour intervals are 2 m.

References

Barberi, F., Bertagnini, A., Landi, P. and Principe, C. (1992) A review on phreatic eruptions and their precursors. *J. Volcanol. Geotherm. Res*., **52**, 231–246.

Danhara, T., Yamashita, T., Iwano, H. and Kasuya, M. (1992) An improved system for measuring refractive index using the thermal immersion method. *Quaternary International*, **13/14**, 89–91.

Goto, Y. and Danhara, T. (2011) Zircon fission-track dating of the Hiyoriyama Cryptodome at Kuttara Volcano, southwestern Hokkaido, Japan. *Bull. Volcanol. Soc. Japan*, **56**, 19–23.

Goto, Y. and Johmori, A. (2011) Controlled source audio-frequency magnetotelluric (CSAMT) and time domain electro-magnetic (TDEM) resistivity measurements at Noboribetsu Geothermal Field, Kuttara Volcano, Hokkaido, Japan. *Bull. Volcanol. Soc. Japan*, **56**, 153–160.

Goto, Y. and Johmori, A. (2013) Resistivity structure of the Hiyoriyama Cryptodome at Kuttara Volcano, Hokkaido, Japan. *Bull. Volcanol. Soc. Japan*, **58**, 365–376.

Goto, Y., Matsuzuka, S. and Kameyama, S. (2011a) Three-dimensional digital mapping of Noboribetsu Geothermal Field, Kuttara Volcano, Hokkaido, Japan, using helicopter-borne high-resolution laser scanner. *Bull. Volcanol. Soc. Japan*, **56**, 127–135.

Goto, Y., Sasaki, H., Toriguchi, Y. and Hatakeyama, A. (2011b) A phreatic explosion after AD 1663 at the Hiyori-yama Cryptodome, Kuttara Volcano, southwestern Hokkaido, Japan. *Bull. Volcanol. Soc. Japan*, **56**, 147–152.

Goto, Y., Sasaki, H., Toriguchi, Y. and Hatakeyama, A. (2013) History of phreatic eruptions in the Noboribetsu Geothermal Field, Kuttara Volcano, Hokkaido, Japan. *Bull. Volcanol. Soc. Japan*, **58**, 461–472.

Hayakawa, Y. (1985) Pyroclastic geology of Towada volcano. *Bull. Earthq. Res. Inst*., **60**, 507–592.

Katsui, Y., Yokoyama, I., Okada, H., Abiko, T. and Muto, H. (1988) **Kuttara (Hiyoriyama), its volcanic geology, history of eruption, present state of activity and prevention of disasters**. Committee for Prevention and Disasters of Hokkaido, Sapporo, 99p. (in Japanese)

Machida, H. and Arai, F. (2003) **Atras of tephra in and around Japan**. University of Tokyo Press, Tokyo, 360p. (in Japanese)

McPhie, J., Doyle, M. and Allen, R. (1993) **Volcanic textures**. University of Tasmania, Hobart, 196p.

Moriizumi, M. (1998) The growth history of the Kuttara volcanic group. *Bull. Volcanol. Soc. Japan*, **43**, 95–111. (in Japanese with English abstract)

Ui, T., Nakagawa, M., Inaba, C., Yoshimoto, M. and Geological Party, Joint Research Group for the Usu 2000 Eruption (2002) Sequence of the 2000 Eruption, Usu Volcano. *Bull. Volcanol. Soc. Japan*, **47**, 105–117. (in Japanese with English abstract)

Yamazaki, T. (1986) ^{14}C age of the Oyunuma-Jigokudani explosion deposits, Kuttara volcano, southwestern Hokkaido, Japan. *Earth Science (Chikyu Kagaku)* , **40**, 221–223. (in Japanese)

Yokoyama, Katsui, Y., Oba, Y. and Ehara, Y. (1973) **Usuzan, its volcanic geology, history of eruption, present state of activity and prevention of disasters**. Committee for Prevention and Disasters of Hokkaido, Sapporo, 254 p. (in Japanese)

(Editional handling Yuki Suzuki)

北海道クッタラ火山登別地熱地域の水蒸気噴火: 1663 年以降の活動

後藤芳彦・鳥口能誠・佐々木央岳・畠山　信

北海道クッタラ火山，登別地熱地域の最も新しい水蒸気噴火堆積物 (Nb-a) の調査を行い，その分布域と噴火様式を解明した．調査は登別地熱地域全域の 71 地点で手掘りトレンチ（深度 <90 cm）を掘削して行った．水蒸気噴火堆積物は，最大層厚 68 cm で，変質した岩石片と細粒なマトリクスからなり，有珠山 b 降下軽石（Us-b，西暦 1663 年）を覆う．この水蒸気噴火堆積物は，北北西–南南東に伸長する 850×1250 m の範囲に分布し，その層厚と最大粒径は，複数の爆裂火口（日和山山頂，大湯沼，笠山北，奥の湯，鉄泉池）に向かって増大する．登別地熱地域では，西暦 1663 年以降（17 世紀末～19 世紀ごろ），複数の地点で水蒸気噴火が起き，北北西–南南東方向に配列する複数の火口が形成されたと考えられる．